Electronic Supplementary Material (ESI) for Journal of Materials Chemistry A.

Unconventional structural and morphological transitions of nanosheets, nanoflakes and nanorods of AuNP@MnO_2

Ben Liu,[a] Islam M. Mosa,[a,b] Wenqiao Song,[a] Haoquan Zheng,[c] Chung-Hao Kuo,[a] James F. Rusling,[a,d] Steven L. Suib,*[a,d] Jie He*[a,d]

[a]Department of Chemistry, University of Connecticut, Storrs, Connecticut, 06269, USA
Emails: steven.suib@uconn.edu (SLS) and jie.he@uconn.edu (JH)
[b]Department of Chemistry, Tanta University, Tanta, 31527, Egypt
[c]Berzelii Center EXSELENT on Porous Materials, Department of Materials and Environmental Chemistry, Stockholm University, Stockholm, 10691, Sweden
[d]Institute of Materials Science, University of Connecticut, Storrs, Connecticut, 06269, USA.

Contents

Figure Contents

1. Synthesis of gold nanoparticles (AuNPs)

1.1 Synthesis of AuNPs with a diameter of 4 nm

A 100 mL aqueous solution containing 4.9 mg of $HAuCl_4$ and 3.7 mg of sodium citrate was first mixed in a conical flask. Next, 2 mL of ice-cold, freshly prepared 0.1 M of $NaBH_4$ solution was added to the solution under strong stirring. The solution was further stirred for 3-4 hrs. The average size of obtained AuNPs is ~4 nm. Then, 30 mg of sodium citrate was added the above solution to obtain citrate-protected AuNPs.

1.2 Synthesis of AuNPs with the diameter of 14 nm, 23 nm and 45 nm

For 14 nm AuNP, 100 mg of $HAuCl_4$ was first dissolved in 1 L of water and heated to boiling (100 ^oC) under stirring. 30 mL of sodium citrate solution (1 wt%) was quickly injected. The reaction mixture was then refluxed for 30 min. The average size of obtained AuNPs is ~14 nm. For 23 nm/45 nm AuNPs, 10 mg of $HAuCl_4$ was dissolved in 500 mL of water and heated to boiling (100 ^oC) under stirring. To this solution, 3 mL of sodium citrate solution (1 wt%) was quickly injected. The reaction mixture was then stirred at 100 ^oC for 30 min. The solution was then cooled down to 85 ^oC. Another 3 mL of sodium citrate (1 wt%) solution was quickly injected into the solution, followed by the injection of 1 mL of $HAuCl_4$ solution (1 wt%). By repeating this step for four times/ten times every 15 min, 23 nm/45 nm AuNPs can be prepared.

2. Synthesis of MnO_2 nanocatalysts without AuNPs

20 mL of $KMnO_4$ solution (10 mM) was slowly added dropwise to 80 mL of sodium citrate solution (0.3 mg/mL) under vigorous stirring. The resulting mixture was stirred for 1 h and hydrothermally treated at 80 ^oC for 2 h. The obtained product was washed by water to obtain nanosheets (Figure S13a). The above solution of MnO_2 nanosheets was hydrothermally treated at 160 ^oC for additional 24 h. The product was centrifuged and washed by water to obtain pure MnO_2 nanorods (Figure S13b).

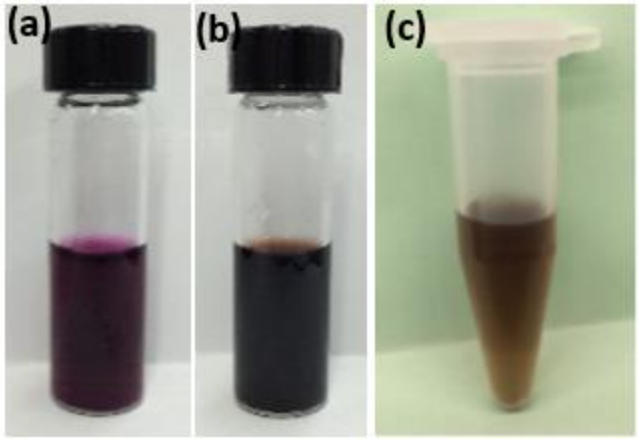

Fig. S1 The optical pictures of reaction mixtures (a) before, (b) after hydrothermal treatment and (c) after centrifugation.

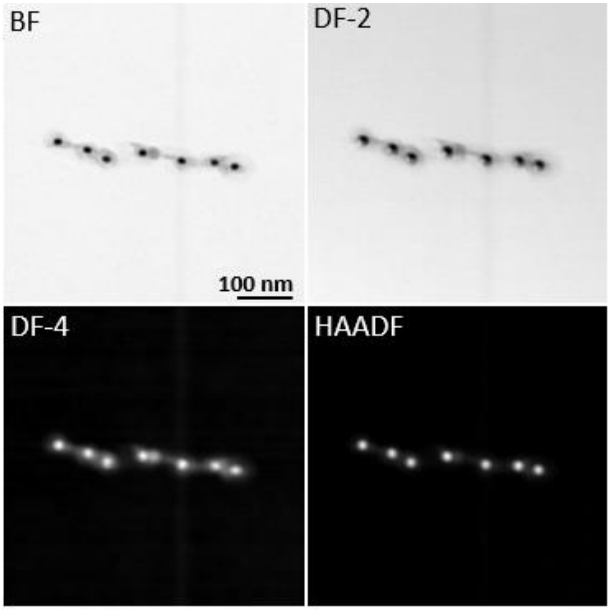

Fig. S2 Bright-field and dark-field STEM images of AuNP@MnO_2 nanosheets, indicating that the monodispersed AuNPs surround with a dense MnO_2 shell with a typical homocentric core-shell nanostructures.

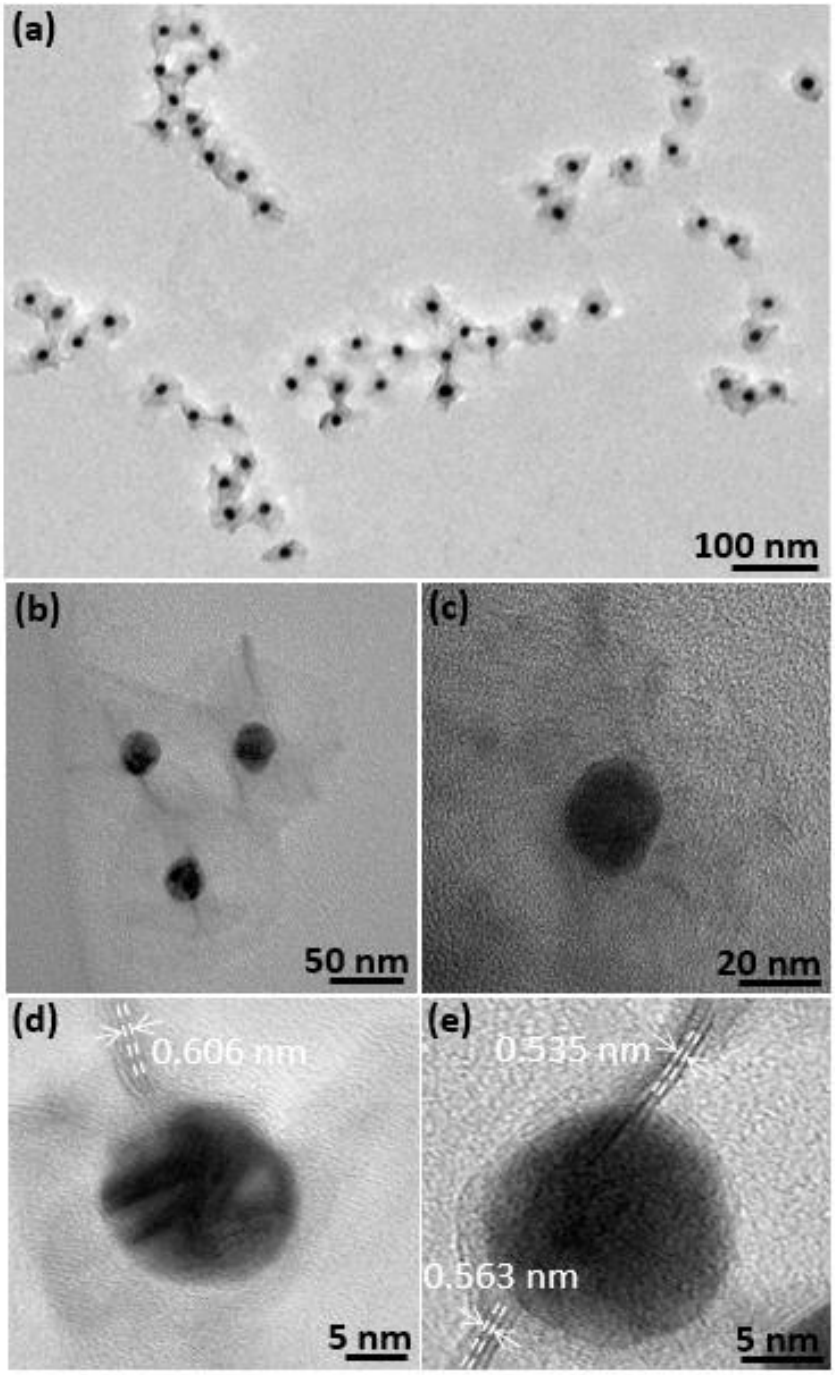

Fig. S3 TEM images (a-c) and high-resolution TEM (d, e) of AuNP@MnO_2 nanosheets shown in Fig. 1, indicating the random lamellar *d*-spacing of nanosheets.

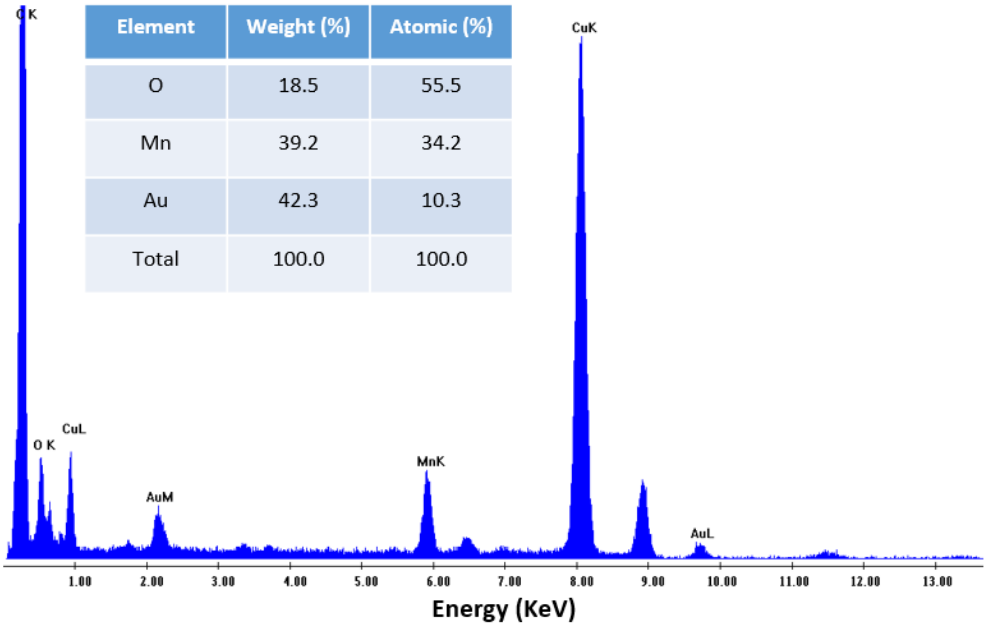

Fig. S4 STEM EDX spectra and corresponding elemental composition (insert) of AuNP@MnO_2 nanosheets.

Table S1 Summary of the weight content of Au in Au@MnO_2 via atomic absorption measurement

Catalysts	**AuNP@MnO_2 nanosheets**	**AuNP@MnO_2 nanoflakes**	**AuNP@MnO_2 curled nanoflakes**	**AuNP@MnO_2 nanorods**
Weight Percentage (Au)	42.6%	41.5%	41.9%	39.7%

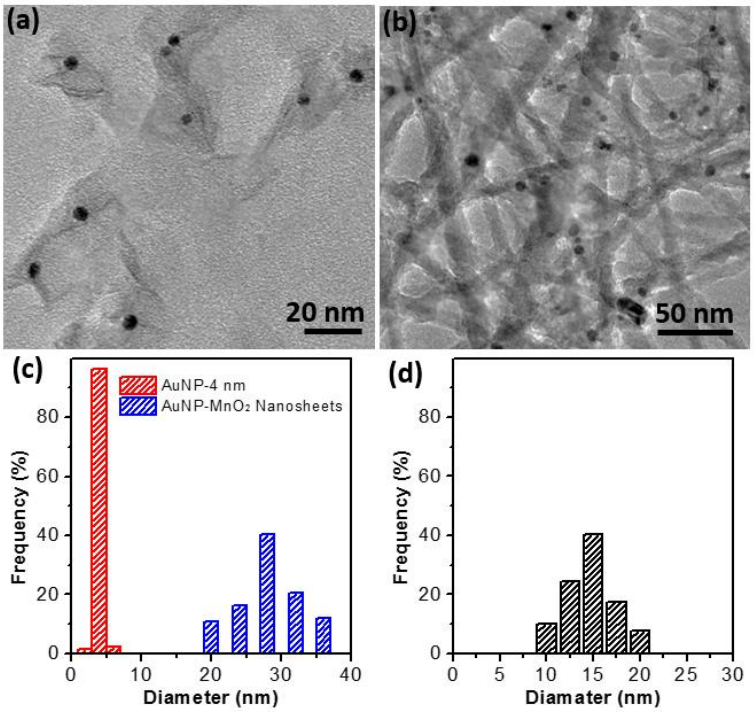

Fig. S5 The morphologies and structures of AuNP (4 nm)@MnO_2 nanosheets and nanorods. TEM images of AuNP (4 nm)@MnO_2 nanosheets (a) and nanorods (b). (c) The size distributions of AuNPs and nanosheets shown in Fig. S5a, and (d) the diameter distribution of nanorods shown in Fig. S5b.

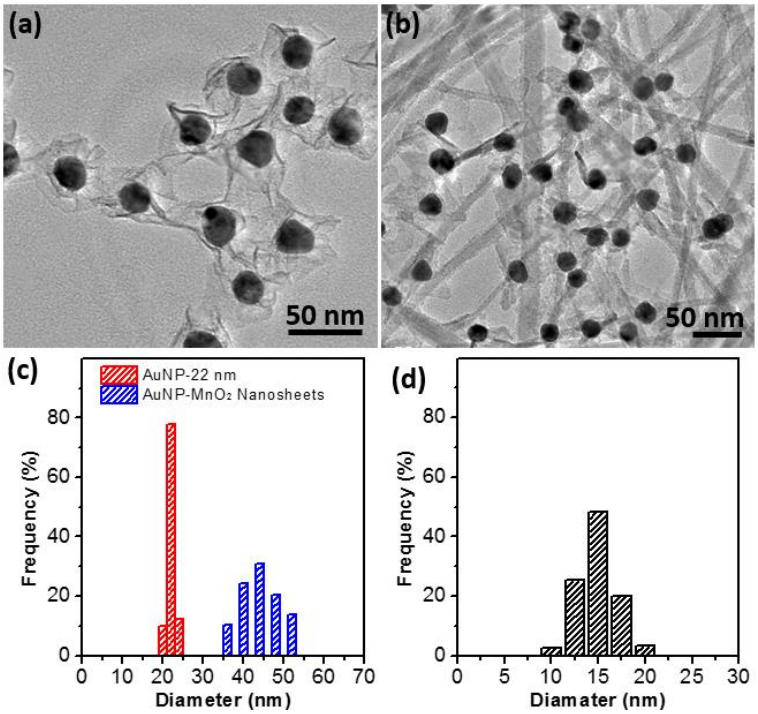

Fig. S6 The morphologies and structures of AuNP (22 nm)@MnO_2 nanosheets and nanorods. TEM images of AuNP (22 nm)@MnO_2 nanosheets (a) and nanorods (b). (c) The size distributions of AuNPs and nanosheets shown in Fig. S6a, and (d) the diameter distribution of nanorods shown in Fig. S6b.

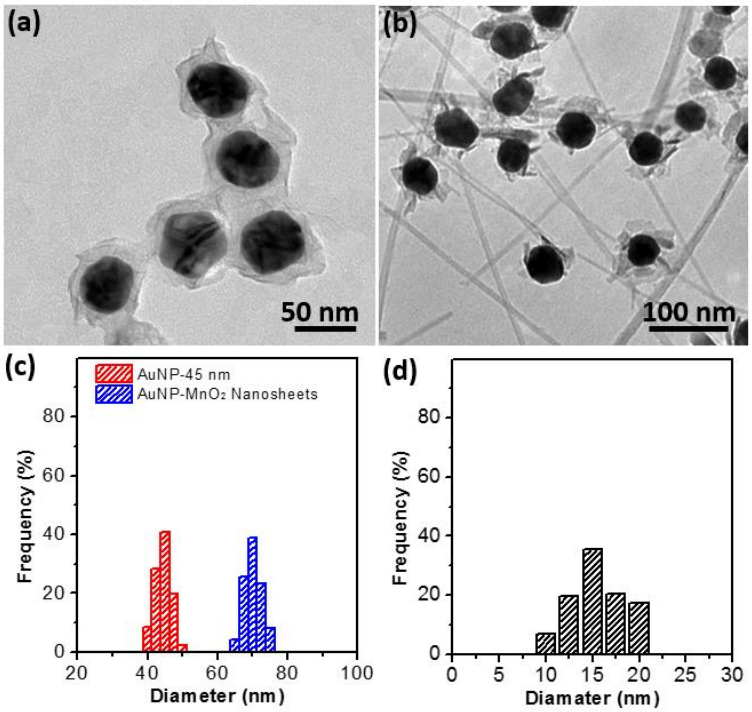

Fig. 7 The morphologies and structures of AuNP (45 nm)@MnO_2 nanosheets and nanorods. TEM images of AuNP (45 nm)@MnO_2 nanosheets (a) and nanorods (b). (c) The size distributions of AuNPs and nanosheets shown in Fig. S7a, and (d) the diameter distribution of nanorods shown in Fig. S7b.

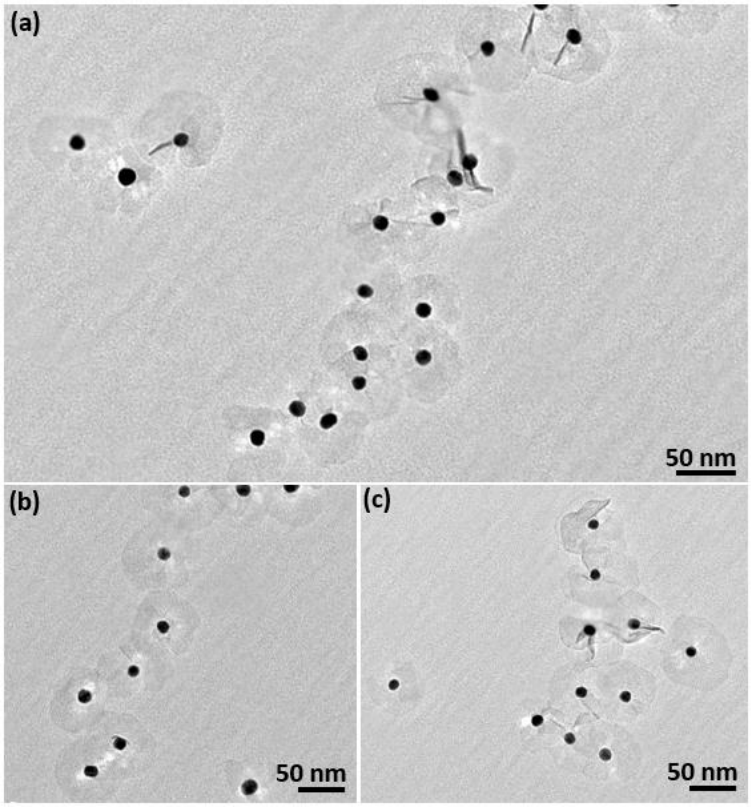

Fig. S8 Supplementary TEM images (a-c) of AuNP@MnO_2 nanoflakes shown in Fig. 2a.

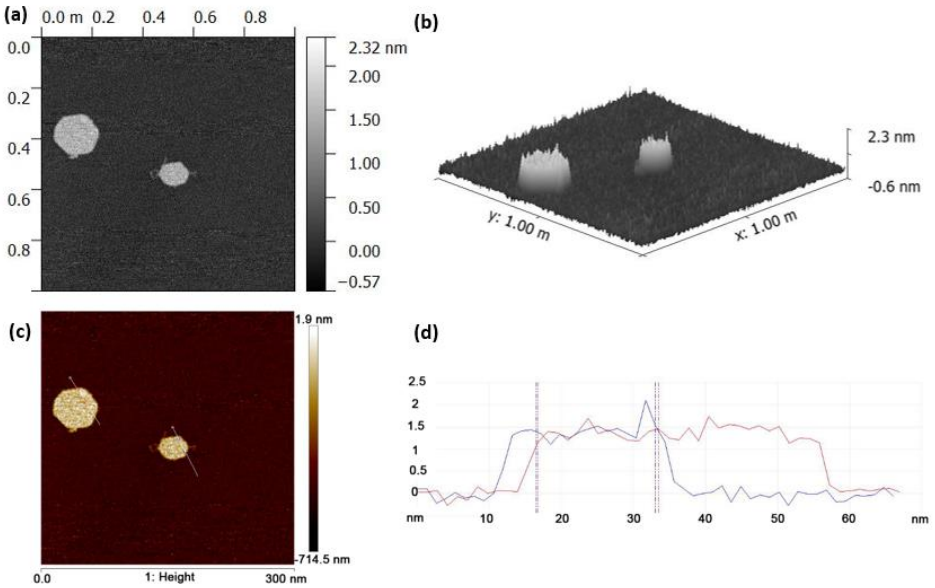

Fig. S9 AFM images of AuNP@MnO_2 nanoflakes. The thickness of nanoflakes from AFM images is ~1.4 nm, clearly indicating only 2~3 layers of MnO_2 single nanosheets presented in nanoflakes.

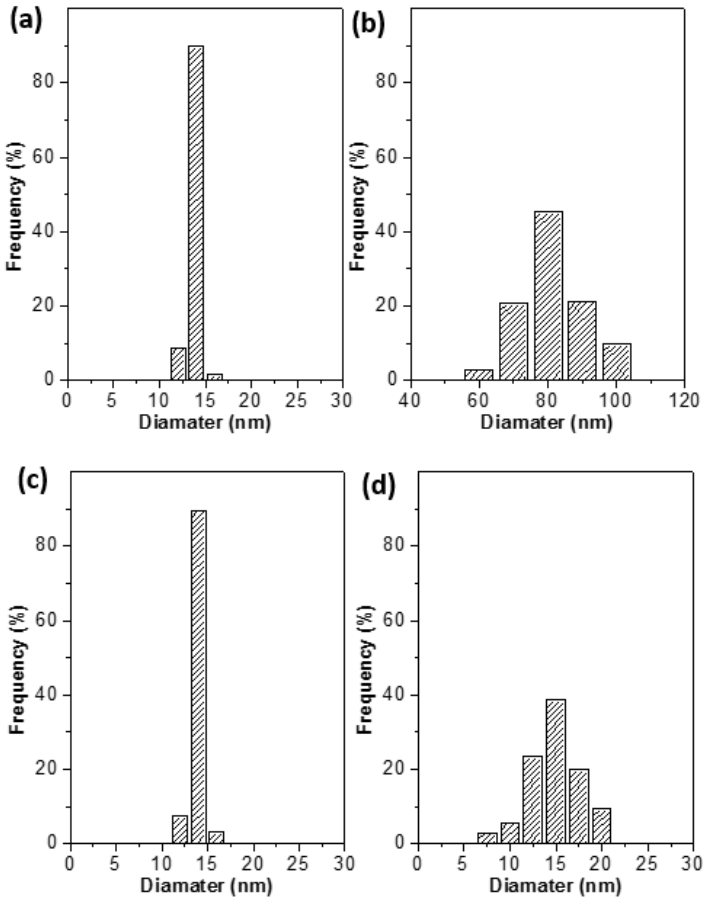

Fig. S10 Size distributions of AuNP@MnO_2 nanocatalysts. The diameter of AuNPs (a) and total nanoflakes (b) for AuNP@MnO_2 nanoflakes shown in Fig. 2a, and the diameter of AuNPs (a) and MnO_2 rods (b) for AuNP@MnO_2 nanorods shown in Fig. 2e.

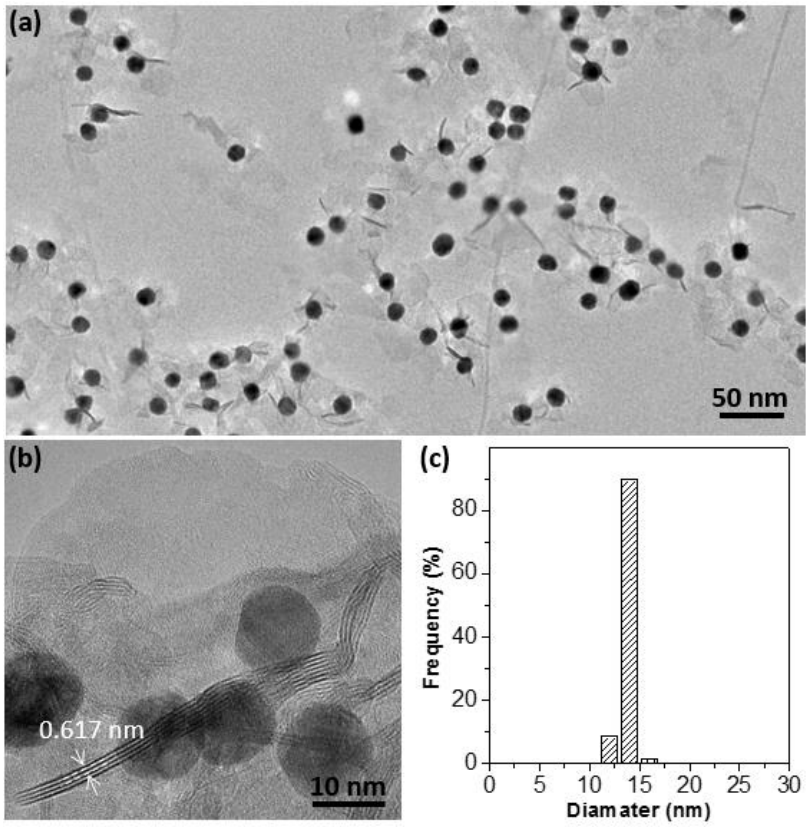

Fig. S11 (a, b) Supplementary TEM images of curled AuNP@MnO_2 nanoflakes shown in Figure 2c. (c) Size distribution of the diameter of AuNPs in curled AuNP@MnO_2 shown in Fig. 2c.

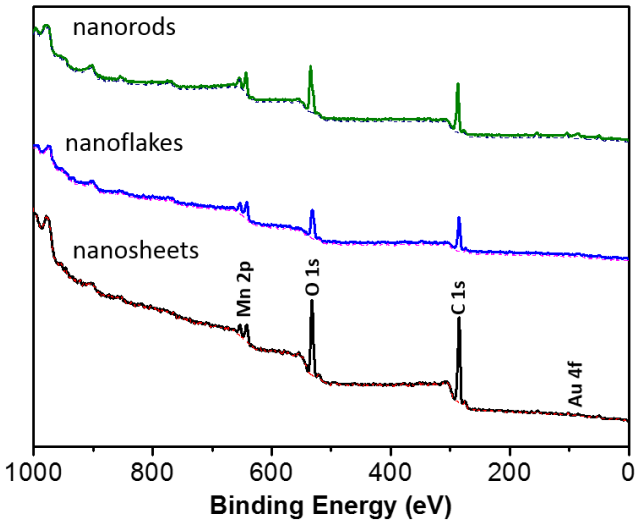

Fig. S12 XPS spectra of AuNP@MnO_2 catalysts. The results indicate that the catalysts contain Mn, Au and O elements.

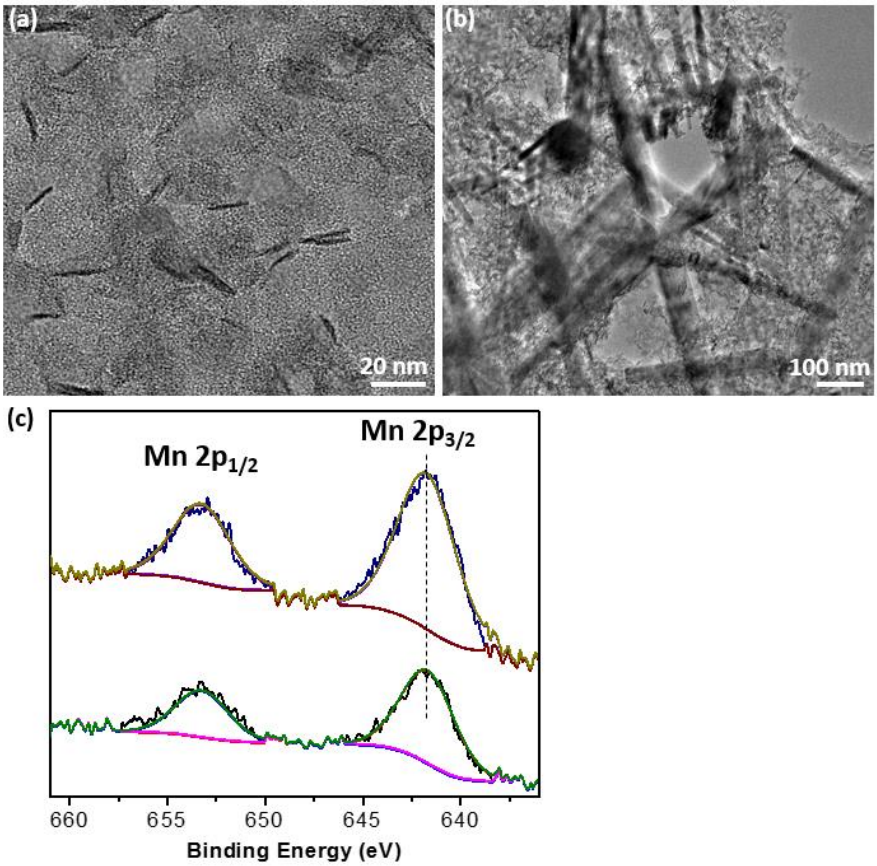

Fig. S13 The morphologies and structures of MnO_2 nanosheets (a) and nanorods (b) synthesized using $KMnO_4$ as Mn source and sodium citrate as reducing agent. XPS spectra (c) of MnO_2 nanosheets and nanorods shown in Fig. S13a and b. The signals of Mn 2p did not change, indicating no change in oxidation state between Mn^{3+} and Mn^{4+} in the absence of AuNPs.

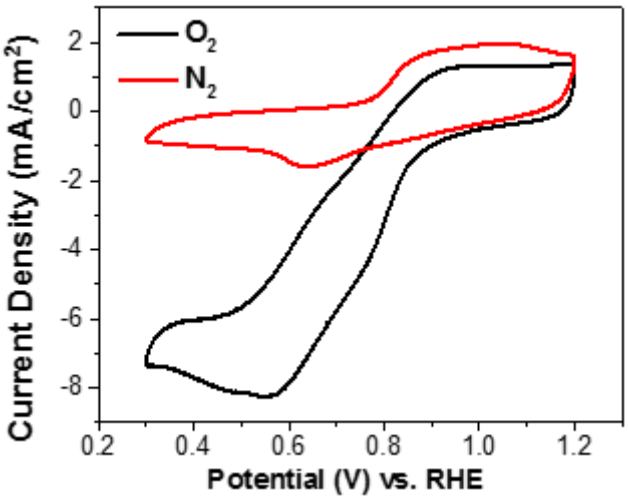

Fig. S14 CV scans of AuNP@MnO_2 nanosheets in N_2- and O_2-saturated 0.1 M KOH solution. The CV curves were taken under rotation at 1600 rpm in both O_2-saturated and N_2-saturated 0.1 M KOH at a scan rate of 10 mV/s.

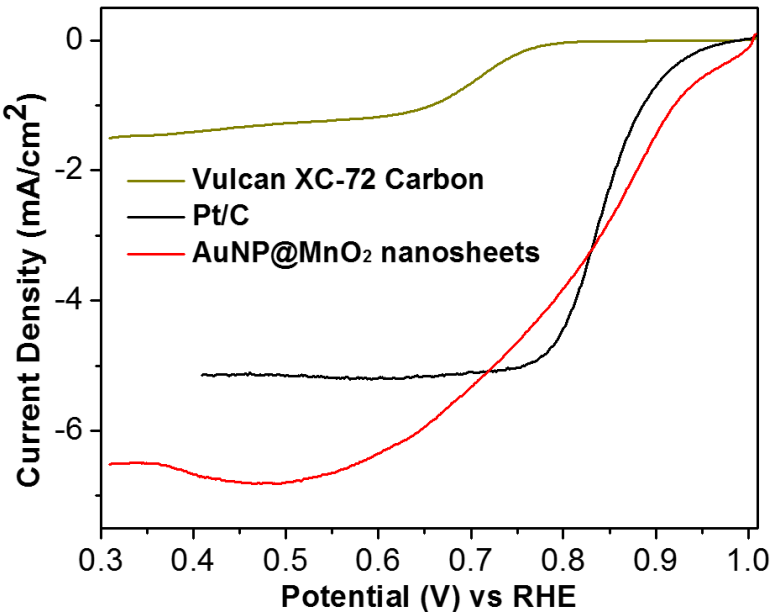

Fig. S15 ORR activity of Vulcan XC-72 carbon black. The ORR activity of carbon support is negligible, compared to that of Pt/C and AuNP@MnO_2 nanosheets,

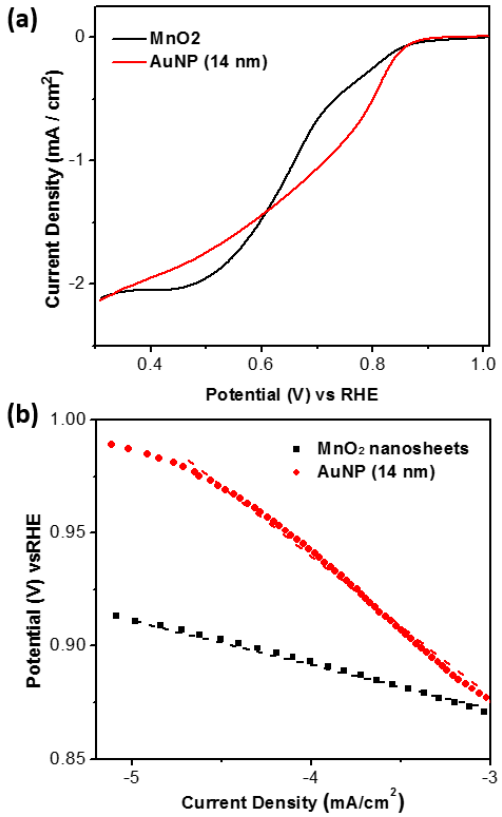

Fig. S16 ORR activities (a) and Tafel plots (b) of pure MnO_2 nanosheets (black line) and AuNPs (14 nm) (red line). Both of them show the poor ORR activity, compared to that of AuNP@MnO_2 nanosheets. The rotation speed of electrodes is 1600 rpm and the loading amount is 0.24 mg/cm^2.

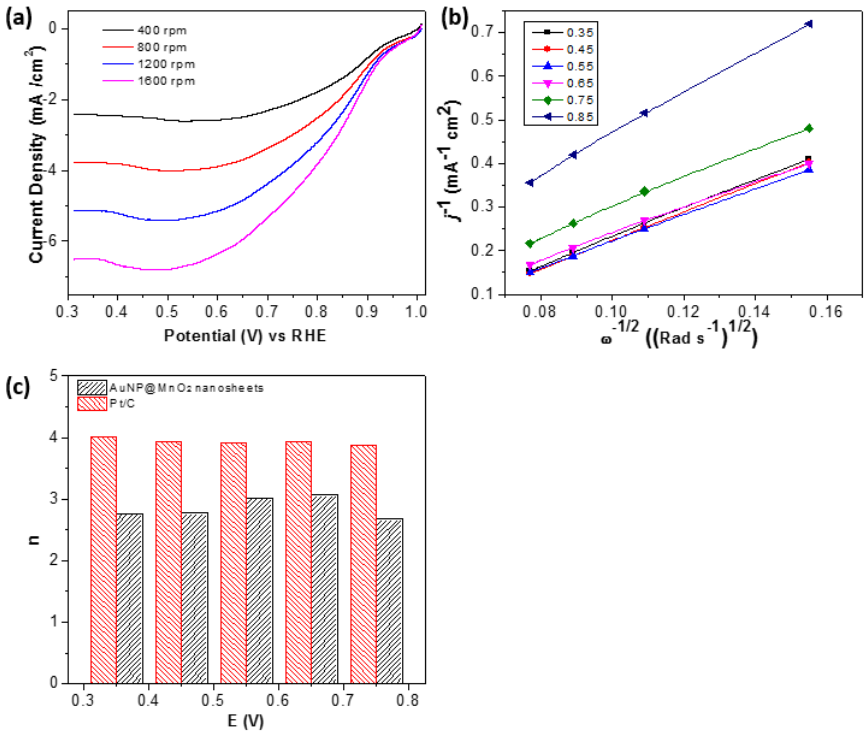

Fig. S17 LSV curves of AuNP@MnO_2 nanosheets at various rotating rates (a) and corresponding K-L plots (b), and (c) the electron transfer number (n) of AuNP@MnO_2 nanosheets and Pt/C at different potentials. The rotation speed of electrodes is 1600 rpm and the loading amount is 0.24 mg/cm^2.

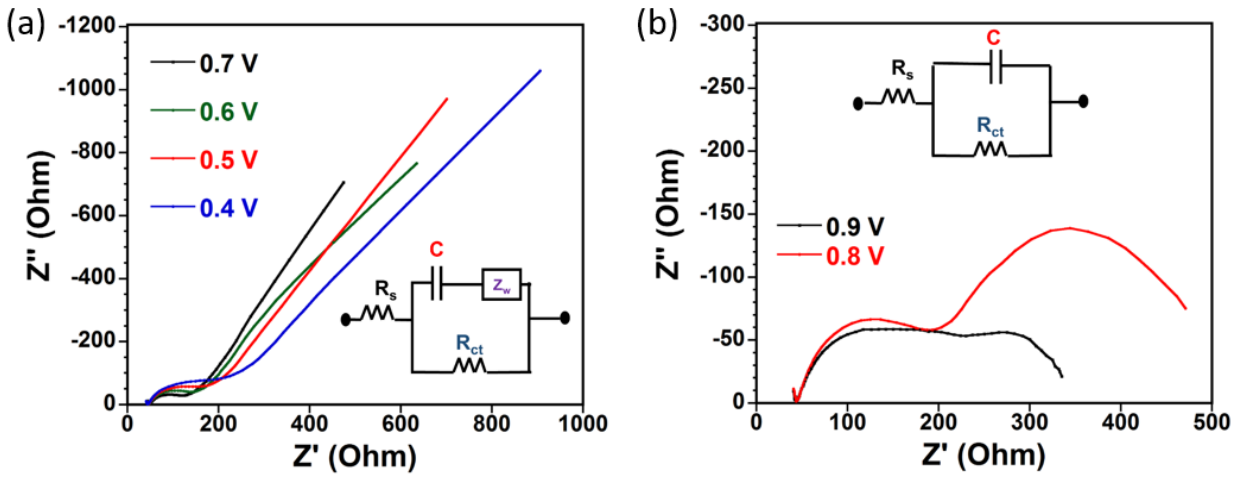

(c)

E (V)	R_{ct} (Ω)	k^o (cm s^{-1})	E (V)	R_{ct} (Ω)	k^o (cm s^{-1})
0.9	265	0.0067	**0.6**	300	0.0058
0.8	667	0.0026	**0.5**	438	0.0039
0.7	215	0.0080	**0.4**	711	0.0025

Fig. S18 (a,b) Electrochemical impedance spectroscopy (EIS) analysis at different potentials in volts vs. RHE for Au-MnO_2 nanosheets. The inset shows the fitted equivalent circuit for the EIS spectra. Z` and Z`` represent the real and imaginary parts of the impedance values respectively. R_s, R_{ct}, Z_w, and C are solution resistance, charge transfer resistance, diffusion element, and capacitance, respectively. (c) Table of heterogeneous electron transfer rate constant at various potentials. The k^o value was calculated by assuming the average number of electrons transferred, n = 3.

At high potentials (0.8-0.9 V vs. RHE), Nyquist plots of the EIS curves are limited to the kinetically controlled region where the reaction mechanism is mainly dependent on the electron transfer rate. At potentials from 0.4-0.7 V vs. RHE, using values of R_{ct} (opposition of electron movement) obtained from the fitted equivalent circuit, the heterogeneous electron transfer rate constant was obtained.

$$J_0 = \frac{i_0}{A} = \frac{R\,T}{n\,A\,F\,R_{ct}}$$

$$k^o = \frac{i_0}{n\,F\,C}$$

where J_0 is the exchange current density A is the electrode surface area, i_0 is the exchange current, R is gas constant, T is temperature, n is the number of electrons transferred, F is Faraday's constant, C is the saturated concentration of oxygen in 0.1 M KOH.

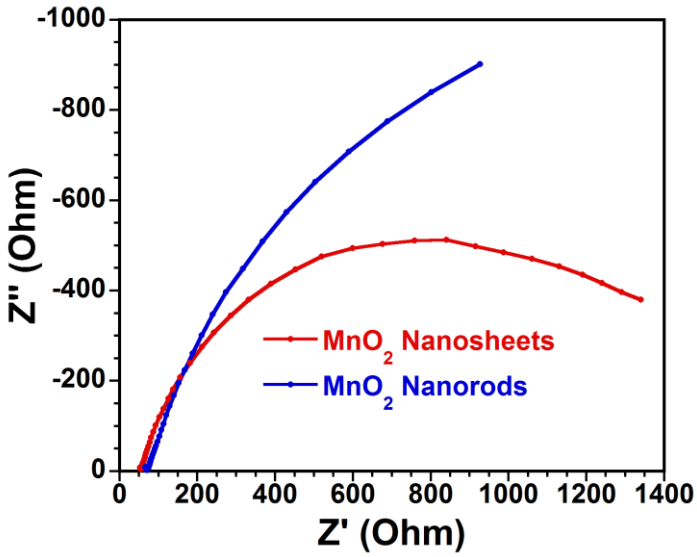

Fig. S19 EIS analysis for MnO_2 nanosheets and nanorods. The charge transfer resistance of MnO_2 nanosheets is 1063 Ohm and the charge transfer resistance of MnO_2 nanorods is ~1515 Ohm.

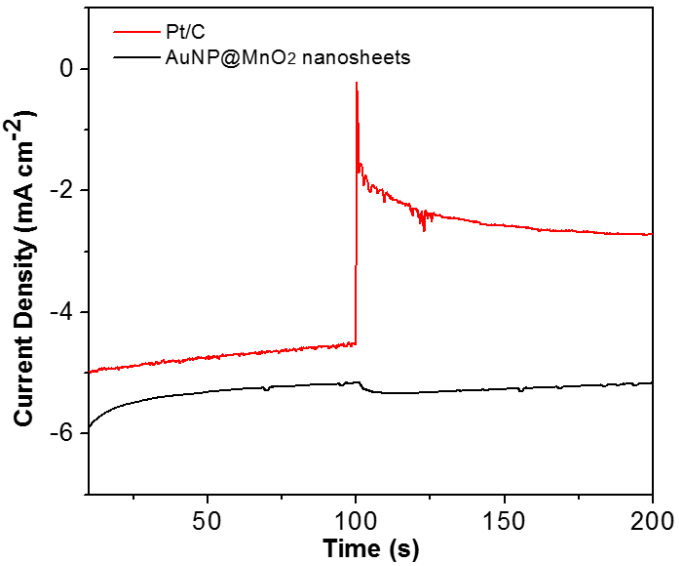

Fig. S20 Methanol crossover effect tests of AuNP@MnO_2 nanosheets (black line) and Pt/C (red line) upon addition of methanol after about 100 seconds in an O_2-saturated 0.1 M KOH solution.